Supporting Information for:

Solubility-Limited Depolymerization Kinetics in the Glycolysis of Carbonyl-Containing Polymers

Shelby Watson-Sanders,[1] Kendra Day Johnson,[1] Sarah Barber,[1] Alison Biery[1], Landri Wilcox,[1] Nicholas J. Galan,[3] Jackie Zheng,[3] Tomonori Saito,[3] Mark Dadmun[1,*]

[1]Chemistry Department, University of Tennessee, Knoxville, TN 37996

[2]National Renewable Energy Laboratory, Golden, CO

[3]Oak Ridge National Laboratory, Oak Ridge, TN

* Corresponding Author (Dad@utk.edu)

Table of Contents

Methods

Nuclear Magnetic Resonance (NMR)

In the NMR analysis, the PET, PETG, and subsequent oligomers (30-60 mg) were dissolved in HFIP (1 mL). The sample:HFIP mixture was agitated for five days before 100 microliters of the mixture were mixed with 600 microliters of $CDCl_3$. PC and depolymerized PC (30-60 mg) were mixed with 600 microliters of $CDCl_3$. The NMR data were obtained using a JEOL 400 YH NMR at 35 °C for 160 scans to ensure the sample did not precipitate from solution. The number-average molecular weights (M_n) of the depolymerized PET products were determined using the analysis outlined by Falkenstein.[1] Virgin and depolymerized PET and PETG show peaks at 8.0 ppm (4H, terephthalic protons), 4.65 ppm (4H, methylene protons), and 4.01 ppm (2H, methylene protons on the alpha carbon to the hydroxyl end group). PC and depolymerized PC have peaks at 7.05-7.25 ppm (8H, aromatic protons), 1.72 ppm (6H, methylene protons), and 1.7 ppm (6H, end group methylene protons).[2]

Intrinsic Viscosity molecular weight, M_v

The viscosity average molecular weight of the depolymerization products is measured using a Schott instrument Kapillarviskosimetr 531-10. In this process, PET samples (90-100 mg) are dissolved in 15 mL of HFIP for five days before measuring their intrinsic viscosity (IV). The samples are then equilibrated in the viscometer at 25 ºC for 5 minutes prior to viscosity measurement. Flow times of the PET solution through the viscometer are recorded in quadruplicate at each concentration to assess concentration dependence. After gathering four trial times, the sample is diluted, re-equilibrated, and tested again to obtain additional flow time data. Reduced and inherent viscosities at each concentration are calculated from the flow times using **Equation S1-5**. Intrinsic viscosity is determined from the y-intercept of plots of reduced and inherent viscosity versus concentration. The viscosity average molecular weight (M_v) of PET is then

derived using the Mark-Houwink equation (**Equation S6**), with k and α values of 0.00052 dL/g and 0.695, respectively.[3,4]

Equation S1 Relative Viscosity $$n_{rel} = \frac{t}{t_0}$$

Equation S2 Specific Viscosity $$n_{sp} = \frac{t - t_0}{t_0} = n_{rel} - 1$$

Equation S3 Reduced Viscosity $$n_{sp} = \frac{t - t_0}{t_0 * c} = \frac{n_{sp}}{c}$$

Equation S4 Inherent Viscosity $$n_{sp} = \ln \frac{\frac{t}{t_0}}{c} = \left(\frac{\ln (n_{rel})}{c}\right)$$

Equation S5 Intrinsic Viscosity $$[n] = \lim_{c \to 0} \left(\frac{n_{sp}}{c}\right) = \lim_{c \to 0} \left(\frac{\ln (n_{rel})}{c}\right)$$

Equation S6 Mark-Houwink $$\eta = k{M_v}^{\alpha}$$

Differential Scanning Calorimetry (DSC)

The Differential Scanning Calorimetry (DSC) Q200 curves of the depolymerization product (3-7 mg) were measured in a Hermetic aluminum pan. In the DSC run, the sample was equilibrated at 50 °C before being heated to 280 °C for Polyethylene Terephthalate (PET) and 350 °C for Polyethylene Terephthalate Glycol (PETG) with a ramp of 10 °C/min. PET was heated to 280 °C as literature has shown PET melts at 260 °C.[5,6] PETG was heated to 350 °C to ensure no melting peak past PET's melting curve. However, we didn't expect a melting curve for PETG as it is amorphous.[7] This ramp rate was chosen to inhibit recrystallization during scanning.[8] Enthalpies of melting of the PET samples were determined by measuring the heat flow associated with the melting of PET from the first cycle.[9] The percent crystallinity of each sample was

calculated by dividing the enthalpy of the melting of a PET sample by the enthalpy of 100% crystalline PET (140 J/g).[10]

Fourier Transform Infrared Spectroscopy (FTIR)

FTIR was utilized to evaluate the heterogeneous process and confirm the swelling index of the polymer flake. The FTIR was set to 64 scans to acquire smooth spectra of both the flake and powder. As such, the reaction powder and flake were scanned separately in triplicate, with a background measured between every 5 scans. The instrument's sample holder was cleaned and dried with isopropyl to prevent contaminated and inaccurate readings.

Normalized Swelling [%] for BPA

Half a gram of polymer (PET, or PC) was placed in a 100 mL round bottom flask with BPA and stir bar and sealed with septa in a 1:35 molar ratio of polymer to solvent. Samples were mixed and heated in a 180 °C oil bath for various times (10, 15, 20, 30, or 45 minutes, depending on the polymer) following the swelling procedure from Najmi.[11] Swelling times are not as long as previously reported by Najmi to as dissolution of the polymer started to occur before one hour of swelling. After a specific time, the solvent was decanted hot from the vial and rinsed with methanol for 15 minutes. Then, the methanol was decanted, rinsed again for another 15 minutes, and repeated. The samples were heated at 75 °C for 72 hours to evaporate off the remaining methanol before being weighed. Very quickly, both polymers had a BPA soluble and BPA insoluble fraction, where the BPA soluble polymers dissolute from the polymer flake. This made it more complex to calculate normalized swelling and required us to calculate the amount of BPA diffused into the polymer flake and the amount of insoluble polymer. The amount of BPA gained was calculated using **Equation 2**, where m_f is the final mass (BPA soluble and insoluble), m_i is the initial mass, and $m_{BPA\ gained}$ is the mass of BPA diffused into the polymer flakes. The amount of polymer remaining that was BPA insoluble ($m_{polymer}$) was calculated using **Equation 3**, where $m_{final\ pellet}$ is

the final mass, not including BPA soluble polymer (powder $m_{BPA\ gained}$ is the mass of BPA diffused into the polymer flakes. **Equation 4** combines different swelling ratio equations and **Equations 2 and 3** to obtain the normalized swelling per polymer flake, as the dimensions of the flakes vary between the two polymers of interest.[11,12] The number of flakes was individually counted, and the data were plotted as the square root of time, following Vlachos et al's work.[11]

$$m_{BPA\ gained} = (m_f - m_i) \quad \textbf{(2)}$$

$$m_{polymer} = m_{final\ pellet} - m_{BPA\ gained} \quad \textbf{(3)}$$

$$Normalized\ Swelling\ [\%]_{BPA} = \frac{\frac{m_{final\ flake} - m_{polymer}}{m_{polymer}}}{\#\ flakes} * 100 \quad \textbf{(4)}$$

Glycolysis with Basic Catalyst

Ethylene Glycol (EG), Triazabicyclodecene (TBD) catalyst, carbonyl-containing polymer (PC, PET or PETG) (20:0.5:1 molar ratio), and stir bar were all placed in a 20 mL reaction vial inside a glovebox, sealed with a septum, and transferred outside the glovebox into a 180 °C oil bath. Previous studies indicate that the glycolysis of PET and PC takes 2 hours and 4 hours, respectively, at 180 °C to reach completion.[13,14] However, these reactions reached completion within 4 minutes. To analyze the evolution of the polymer chains during depolymerization, the reaction was stopped at various reaction times (i.e. 1, 2, 3, 4 minutes), and the products were recovered and characterized as described for the glycolysis reactions utilizing TBD:MSA catalyst.[14] PC and PETG oligomers were analyzed using THF Gel permeation Chromatograph/Size Exclusion Chromatograph (GPC/SEC). PETG and its oligomers were dissolved in THF at 67 °C overnight to ensure dissolution. **Scheme S1** illustrates the glycolysis of the 3 polymers to isolate oligomers.

Scheme S1 Heterogeneous glycolysis reaction of PETG, PET, and PC catalyzed by TBD to create oligomers.

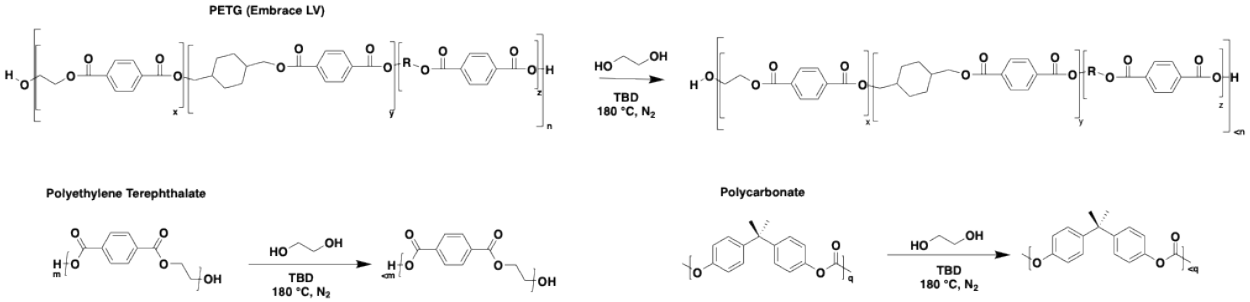

Results

NMR of Starting Material & Products

^{1}H NMR was used to confirm the molecular structures of the isolated oligomers, shown in **Scheme 2**. **Figure S1** shows ^{1}H NMR spectra of virgin PET (green), PET depolymerized with ethylene glycol (EG) (yellow), PET depolymerized with BPA that is BPA-soluble (blue) and BPA-insoluble (purple), and neat BPA (red). **Figure S2** shows ^{1}H NMR spectra of virgin PC (red), PC depolymerized with EG (blue), PC depolymerized with BPA that is BPA-soluble (yellow) and BPA-insoluble (green), and neat BPA (purple). **Figure S3** shows ^{1}H NMR spectra of virgin PETG (red) and PETG depolymerized with EG (blue).

Collectively, these spectra reveal distinct end-group evolution for polyesters versus polycarbonates and for EG versus BPA as depolymerization agents. For PET and PETG depolymerized with EG, we observe an increase in the methylene proton signal at ~4.0 ppm, corresponding to methylene groups α to hydroxyl end groups, consistent with the formation of hydroxyl-terminated polyester chains. In contrast, PC depolymerized with EG exhibits a dominant increase in the methylene protons associated with BPA-based end groups, reflecting that EG more readily undergoes intramolecular ring-closing to form ethylene carbonate than remains as a hydroxyl end group.[13,15] This ring-closing step leaves a phenolic end group on the polymer, attached to the BPA unit in the BPA-based polycarbonate, thereby enriching BPA-terminated

chain ends. When both polyesters and polycarbonates are depolymerized with BPA, all systems show an increase in BPA-based end groups.[16] Notably, **Figure S1** shows that PET depolymerized with BPA does not display a corresponding increase in the ~4.0 ppm methylene signal for α-hydroxyl end groups, indicating a strong preference for BPA attachment and persistence as the dominant chain-end functionality.

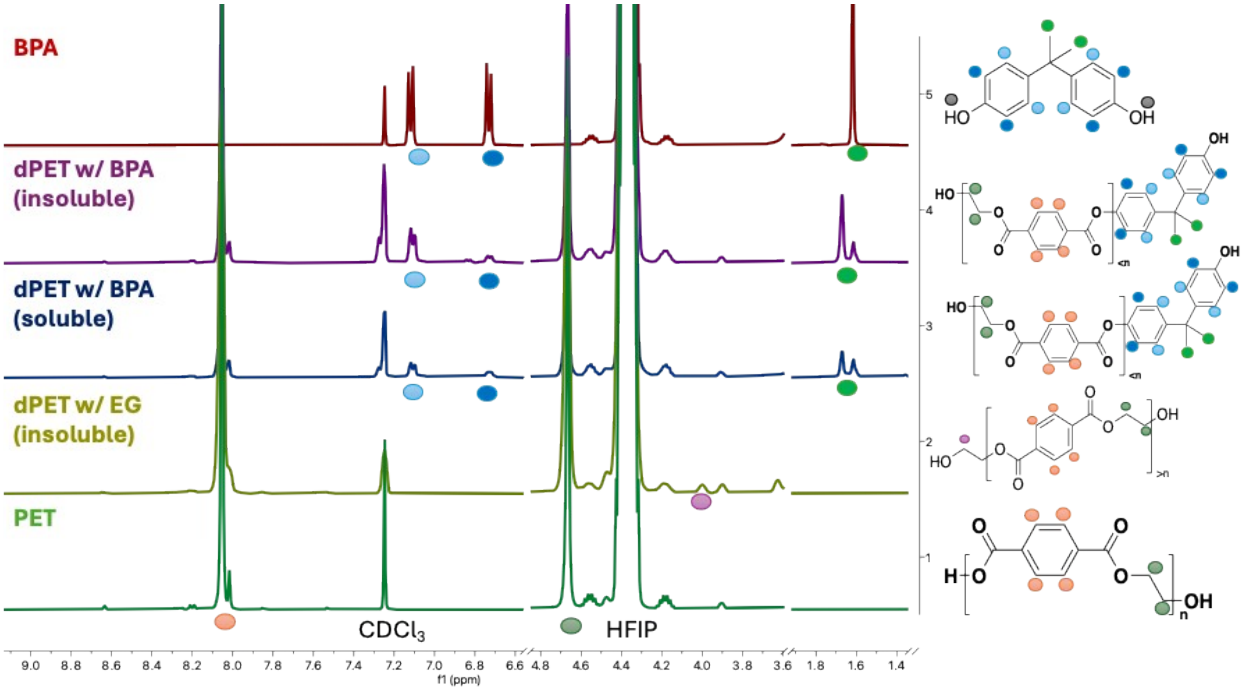

Figure S1 ^{1}H NMR spectra (HFIP:$CDCl_3$) of virgin PET and depolymerized PET products, shown from bottom to top: virgin PET (green), PET depolymerized with ethylene glycol (yellow) showing the appearance of methylene proton signal at ~4.0 ppm corresponding to methylene groups α to the hydroxyl end groups, PET depolymerized with BPA that is BPA-soluble (blue) and BPA-insoluble (purple) exhibiting aromatic and methylene end-group signals characteristic of BPA-terminated oligomers, and neat BPA (red). This series highlights the evolution of end-group structure during depolymerization and the correspondence of oligomer resonances to those of BPA.

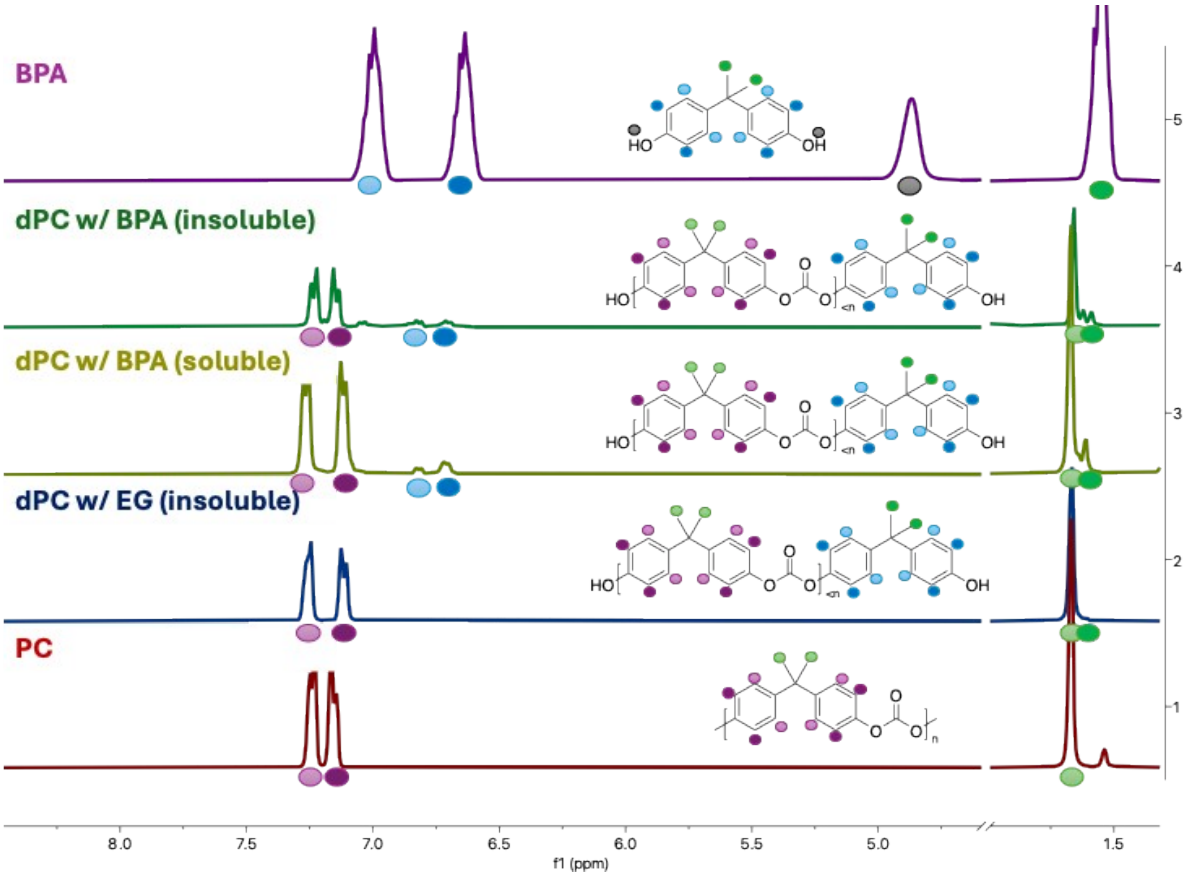

Figure S2 ^{1}H NMR spectra ($CDCl_3$) of virgin PC and depolymerized PC products, shown from bottom to top: virgin PC (red), PC depolymerized with ethylene glycol (blue) displaying a slight increase in methylene proton intensity consistent with BPA-based end groups, PC depolymerized with BPA in the BPA-soluble (yellow) and BPA-insoluble (green) fractions both exhibiting a pronounced increase in methylene resonances arising from BPA-terminated chains, and neat BPA (purple). These spectra illustrate the evolution of BPA-derived end groups during depolymerization and their correspondence to the neat BPA reference.

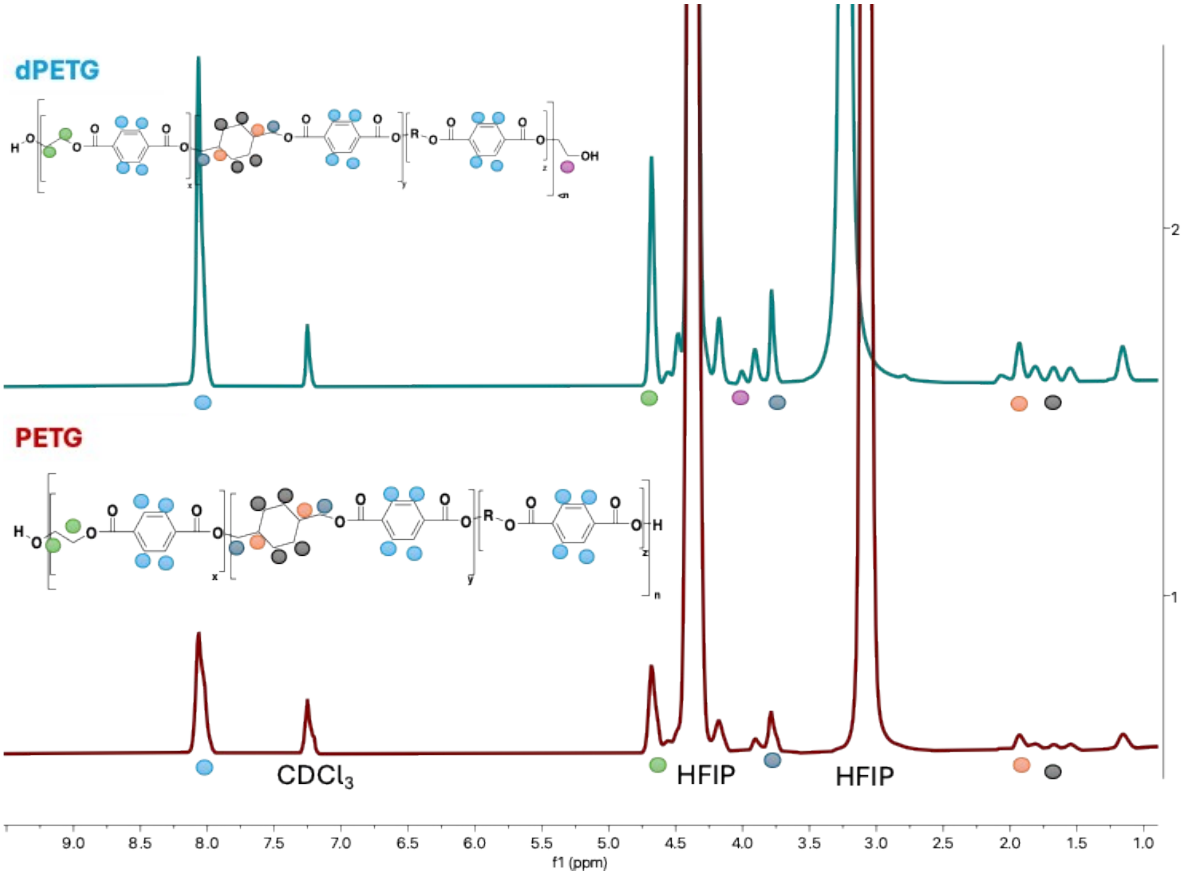

Figure S3 ^{1}H NMR spectra (HFIP:$CDCl_3$) of virgin PETG and PETG depolymerized with ethylene glycol, shown from bottom to top: virgin PETG (red) and PETG depolymerized with ethylene glycol (blue), which exhibits an increase in the methylene proton signal at ~4.0 ppm corresponding to methylene groups α to the hydroxyl end groups. These spectra highlight the growth of hydroxyl-terminated chain ends upon depolymerization.

Absolute molecular weight determination

PET and PETG were depolymerized with EG and PET was depolymerized with BPA, which lasted between 0 and 75 minutes. The decrease in the molecular weight of PET and PETG during depolymerization is assessed using absolute methods, such as Size Exclusion Chromatography (SEC) with light scattering or viscosity measurements. Viscosity measurements yield an absolute molecular weight, the viscosity molecular weight (M_v), which can be compared with the weight-average molecular weight (M_w) obtained from SEC. Ideally, these values (M_v and M_w) should be comparable.[3] **Figure S4** shows variations in M_w and M_v across all depolymerization times. Specifically, **Figure S4 a)** displays the M_v (light purple square) and M_w (purple circle) of

PET depolymerized with EG, tracking changes over time; **b)** shows the M_v (light green square) and M_w (green circle) of PETG depolymerized with EG; **c)** depicts the M_v (light orange square) and M_w (orange circle) of PET depolymerized with BPA. Overall, **Figure S4** demonstrates the comparability of M_v and M_w, providing an additional approach to evaluate changes in PET molecular weight throughout the glycolysis process. **Figure S4** shows that, despite variations in reaction conditions (polyester or nucleophile) and depolymerization times, M_w and M_v remain consistently similar. This consistency underscores the validity of both methods for assessing molecular weight, indicating that it can be reliably applied across various processing conditions.

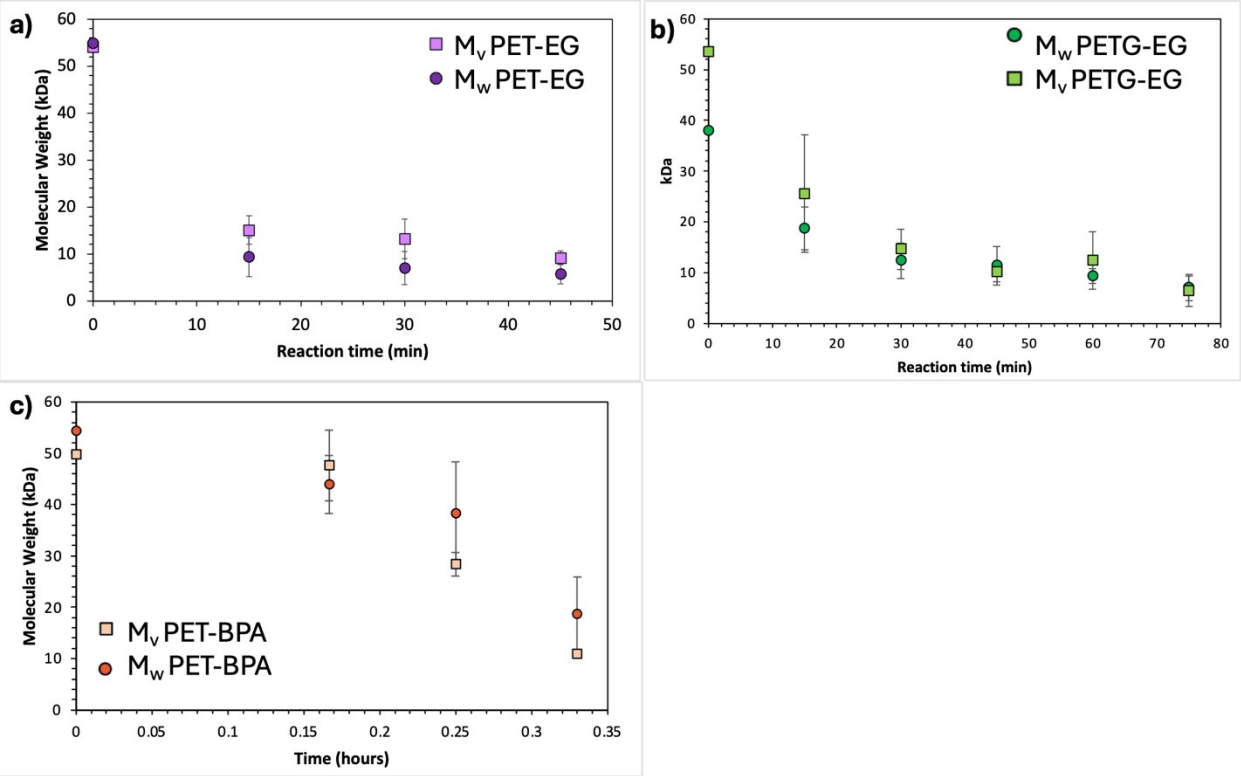

Figure S4 illustrates the variation of molecular weights, M_v and M_w, during the glycolysis of PET, PETG, and PET depolymerized with BPA. **a)** shows M_v (light purple squares) and M_w (purple circles) for PET depolymerized with EG; **b)** presents M_v (light green squares) and M_w (green circles) for PETG depolymerized with EG; and **c)** depicts M_v (light orange squares) and M_w (orange circles) for PET depolymerized with BPA. Each graph illustrates the changes in M_v and M_w with depolymerization time.

Starting Material Characterization

Since Polyethylene Terephthalate Glycol (PETG), Polyethylene Terephthalate (PET), and Polycarbonate (PC) all come from different sources, PETG (Embrace LV) from Eastman Chemical Company and PET and PC from consumer waste, we first characterized the starting molecular weights and crystallinity of the polymers, where the results are shown in **Figure 3** and **Figure S5,** respectively. **Figure S5** shows the heat flow of PC (blue), PET (orange), and PETG (green) vs. temperature. PET has a distinct melting curve starting at 240 °C, which is consistent with the literature. [5,6] There is no melting curve for PC and PETG, as expected. The multiple T_g's that appear in the DSC curve for PETG (68 °C, 113 °C, and 216 °C) could be from the 10 °C/min ramp rate being too fast for PETG. However, T_g values of 68 °C and 113 °C have been reported in the literature and could provide better insight into the copolyester's composition, though this is beyond this project's scope.[7] **Figure S5** verifies that PET is semicrystalline, with a 25% crystallinity, and that PC and PETG are amorphous.

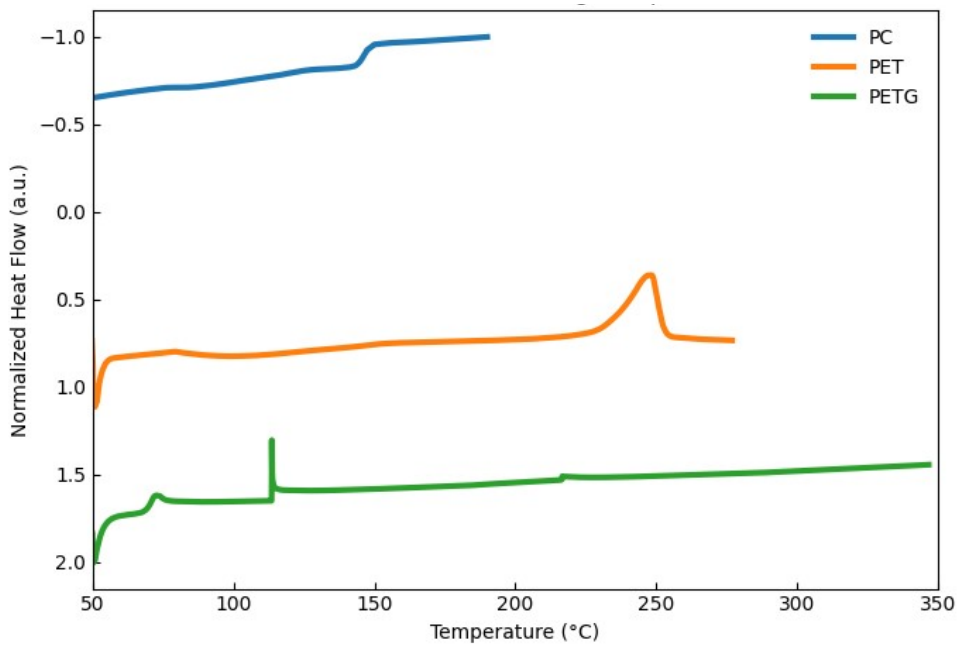

Figure S5 Differential Scanning Calorimetry of polycarbonate (PC, blue), polyethylene terephthalate (PET, orange) and PETG (PET glycol, green) vs. temperature. EXO DOWN

Amphoteric Conditions Depolymerization

Figure S6 presents the depolymerization results of PET, PETG, and PC via glycolysis using TBD:MSA as a catalyst. In **Figure S6 (a),** the yield of EG-insoluble oligomers is shown over time, with PC in orange, PET in blue, and PETG in green. This demonstrates that most oligomeric material remains insoluble in EG during depolymerization. **Figure S6 (b)** provides a visual of the oligomers at the reaction's end: depolymerized PC (dPC) is insoluble in EG, depolymerized PETG (dPETG) is also insoluble with increased turbidity, and depolymerized PET (dPET) displays EG-insoluble oligomer flakes and soluble oligomers, both insoluble in water. This visually represents the transition described in **Figure 1** from a heterogeneous to a coexistence phase during depolymerization, where dPETG shows higher turbidity as some oligomers become EG-soluble, and dPET in water makes the soluble oligomers readily visible as they precipitate out, while insoluble oligomer flakes remain. **Figure S6 (c)** depicts PET depolymerization by showing the change in M_n from NMR spectra of EG-soluble (black) and EG-insoluble (red) oligomers, indicating that at later reaction times, when the transition to the coexistence stage occurs, the molecular weights of soluble and insoluble oligomers become similar as dissolution progresses.

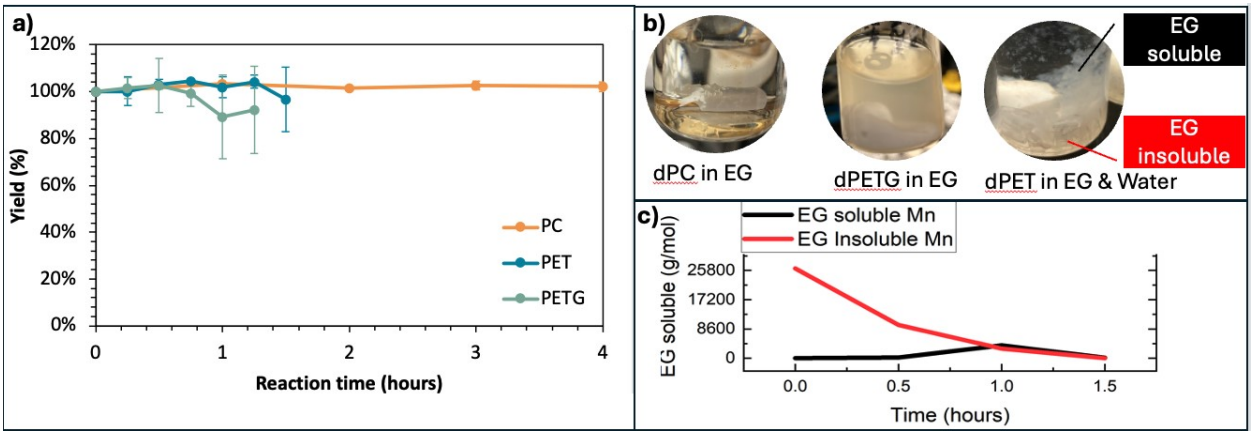

Figure S6. Depolymerization of PET, PETG, and PC via glycolysis using TBD:MSA as a catalyst. **(a)** Yield of EG-insoluble oligomers as a function of reaction time for PC (orange), PET (blue), and PETG (green), showing that the majority of oligomeric material remains insoluble in EG during much of the reaction. **(b)** Representative images of oligomeric products at the end of depolymerization: depolymerized PC (dPC) remains insoluble in EG; depolymerized PETG

(dPETG) is insoluble but exhibits increased turbidity; depolymerized PET (dPET) consists of both EG-insoluble oligomer flakes and EG-soluble oligomers, which precipitate upon transfer to water. These images illustrate the transition from a heterogeneous to a heterogeneous–coexistence depolymerization regime. **(c)** Evolution of number-average molecular weight (M_n), determined by NMR, for EG-insoluble (red) and EG-soluble (black) PET oligomers, showing convergence of molecular weights at later reaction times as dissolution into the EG phase occurs.

Basic Conditions Depolymerization

Figure S7 depicts the results of depolymerizing PET, PETG, and PC via glycolysis using TBD, a very strong base (pKa=26.2), as a catalyst.[17] **Figure S7 (a)** shows reaction vials of PET, PETG, and PC 4 minutes into this glycolysis reaction. As shown in **Figure 8**, PET and PC do not dissolve in EG when the TBD:MSA salt catalyst is used, even after 1.5 and 5 hours, respectively. The lone pair on TBD, not present in TBD:MSA, could enhance the polymer's solubility by acting as a Lewis base, suggesting it may interact with the polymer's polar groups, such as carbonyl or hydroxyl functionalities. These interactions could disrupt intermolecular forces and increase the polymer's compatibility with solvents, potentially aiding in its dissolution.[18-20] **Figure S7 (b)** shows how the percent yield of EG insoluble PETG (orange) and PC (blue) flakes decreases with reaction time. The carbonate-containing polymer solubilizes faster than the ester-containing polymer, which was not previously shown in the EG and BPA reactions utilizing TBD:MSA catalyst. **Figure S7 (c)** shows the percent change in molecular weight of PETG and PC from both the EG soluble and insoluble fractions. **Figure S7 (c)** shows that PC decreases to less than 20% of its original M_n (grey) and M_w (yellow) within 1 minute of the reaction, which takes PETG between 2-3 minutes to reach a similar decrease in M_n (blue) and M_w (orange). **Figure S7 (d)** better illustrates the behavior of the EG insoluble polymer flake by showing M_n (blue for PETG and grey for PC) and M_w (orange for PETG and yellow for PC) with reaction time. Based on the rapid decrease in percent yield and molecular weight of the EG insoluble fraction compared to our previous reactions, we infer that using a suitable catalyst results in higher polymer solubilization,[18-

[21] controlling when the heterogeneous reaction transitions through the three stages of a heterogeneous depolymerization.

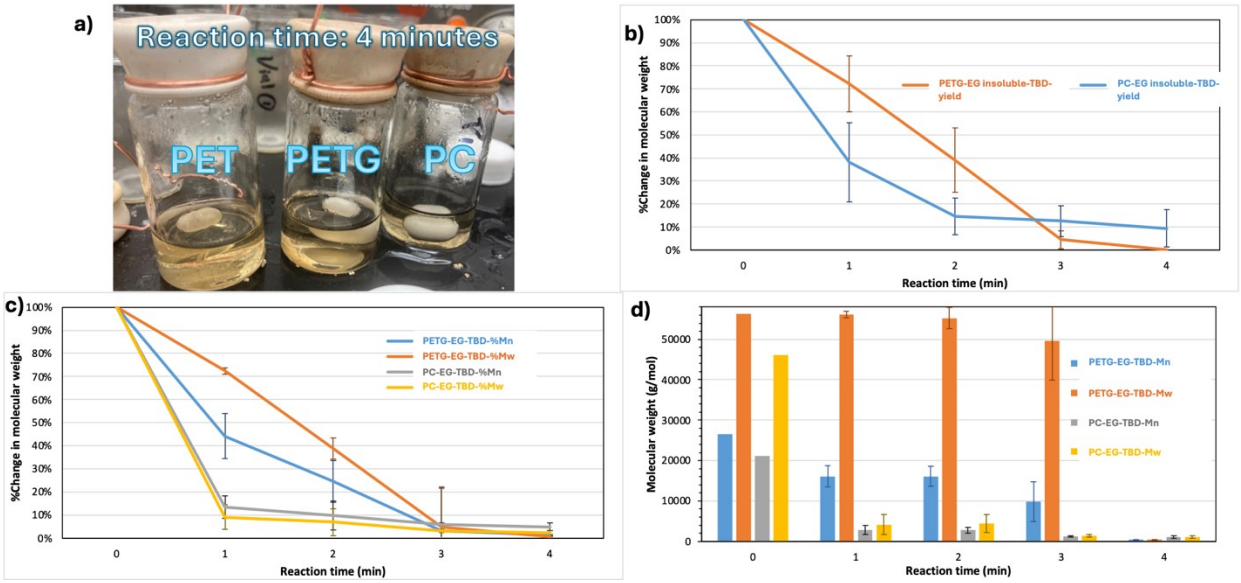

Figure S7 Heterogeneous depolymerization of PET, PETG, and PC via glycolysis catalyzed by TBD. **(a)** Pictures PET, PETG, and PC solubilized in EG:TBD 4 minutes into the reaction. **(b)** shows the percent yield of EG insoluble PETG (orange) and PC (blue) with reaction time. **(c)** Depicts the percent change in molecular weight for PETG (M_n blue, M_w orange) and PC (M_n grey, M_w yellow) of both the EG soluble and insoluble fraction with reaction time. **(d)** Shows the molecular weight of for PETG (M_n blue, M_w orange) and PC (M_n grey, M_w yellow) EG insoluble fraction with reaction time.

Bisphenol-A depolymerization of PET and PC

Figure S8 illustrates macroscopic changes in PC or PET flakes during depolymerization with ethylene glycol (EG) or bisphenol-A (BPA). PET and PC mainly retain their flake shape after long reactions with EG, but PC depolymerized with BPA disperses into BPA, indicating a transition to the coexistence or homogeneous stage. Light purple highlights PET flakes before and after workup with EG, remaining solid and flake-shaped after 1.75 hours. Similarly, dark purple shows PC flakes with EG staying intact after 5 hours. Conversely, blue highlights PC depolymerized with BPA, which loses its flakes after only 0.75 hours. The choice of diol influences the depolymerization stage: BPA causes the oligomeric product to disperse, transitioning from a

heterogeneous to a mixed stage, affecting yield. Figure 9 shows the yield over time for PET and PC depolymerized with BPA, with soluble and insoluble oligomers displayed, highlighting the impact of reaction dynamics on product yield.

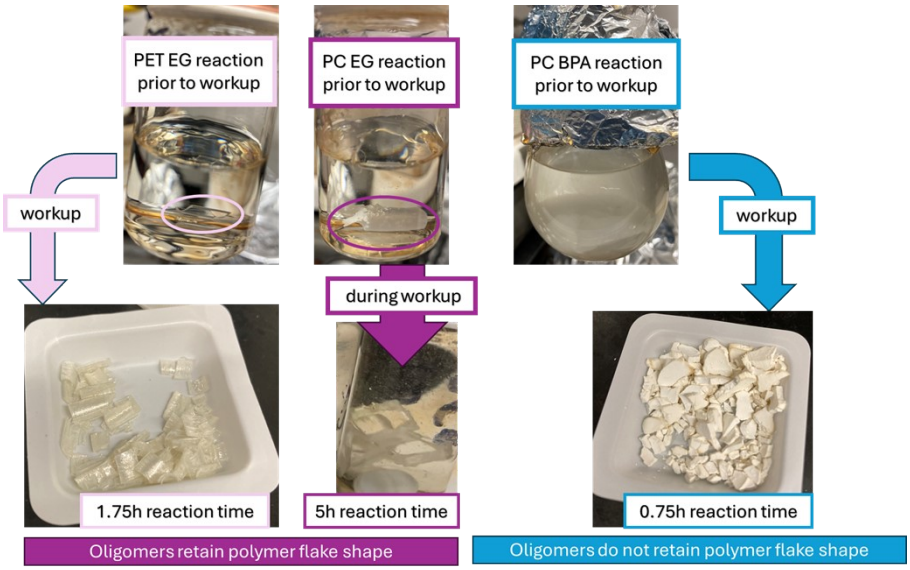

Figure S8 Depolymerization of PET and PC in EG and BPA. Light purple: PET flakes in EG before and after workup (1.75 reaction hours). Dark purple: PC flakes in EG before and after workup (5 reaction hours). Blue: PC flakes in BPA before and after workup (0.75 reaction hours).

We attributed a visual difference in the polymers depolymerized with EG and BPA to swelling and dissolution. **Figure S9** demonstrates how PC experienced swelling and dissolution from EG and BPA. **Figure S9 (a)** shows a visual representation of the diffusion of the solvent into the PC flake. **Figure S9 (b)** shows the change in the PC flakes with depolymerization time in the presence of BPA. Visually, it appeared that the PC flakes became thinner with reaction time. To verify this, we measured the thickness of the PC flakes. **Figure S9 (c)** shows the change in PC flake thickness with reaction time when depolymerized in BPA (purple line) or EG (orange line). PC flakes depolymerized in BPA initially increased in thickness, then decreased to well below the

original thickness of the PC flake. However, the PC flakes depolymerized in EG slowly increased in thickness with reaction time and never decreased despite reacting four times as long as the reactions utilizing BPA.

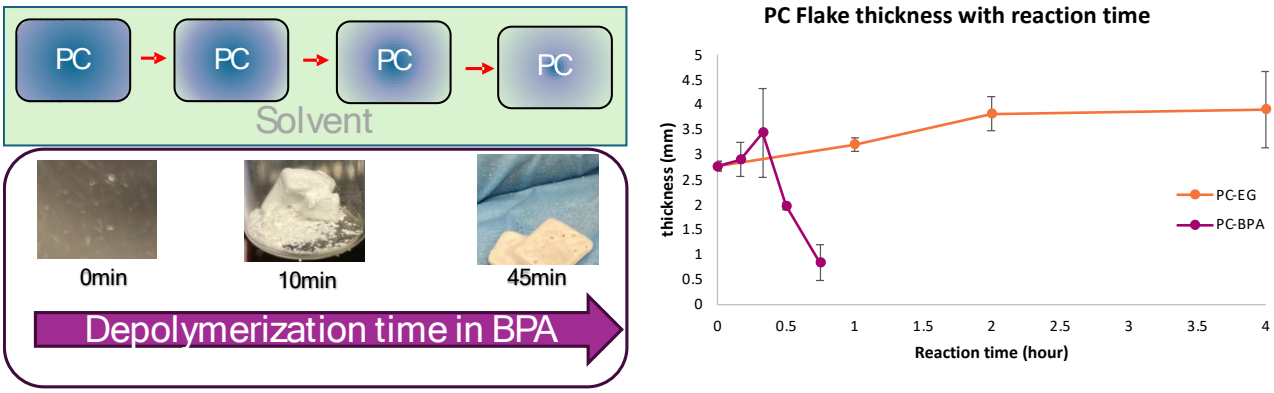

Figure S9 Demonstrates the diffusion of the solvent into the polymer flakes. **(a)** It is a visual signal of solvent (EG or BPA) slowly diffusing into the polymer flake. **(b)** It shows a visual change in PC flakes with depolymerization time in BPA. **(c)** shows a graph of PC flake thickness vs reaction time in EG (orange) and BPA (purple).

Figure S10 shows the total yield of recovered product for both polymers remains high (~100%) throughout the reaction. As the oligomers dissolve into BPA, the yield of BPA insoluble oligomers decreases. Hence, the transition of the reaction from the heterogeneous stage to the coexistence stage and the homogeneous stage decreases the yield of BPA insoluble oligomers with reaction time. A small decrease in the total yield for PC at later reaction times is due to the solubility of smaller PC oligomers and monomer in the methanol used during the workup.

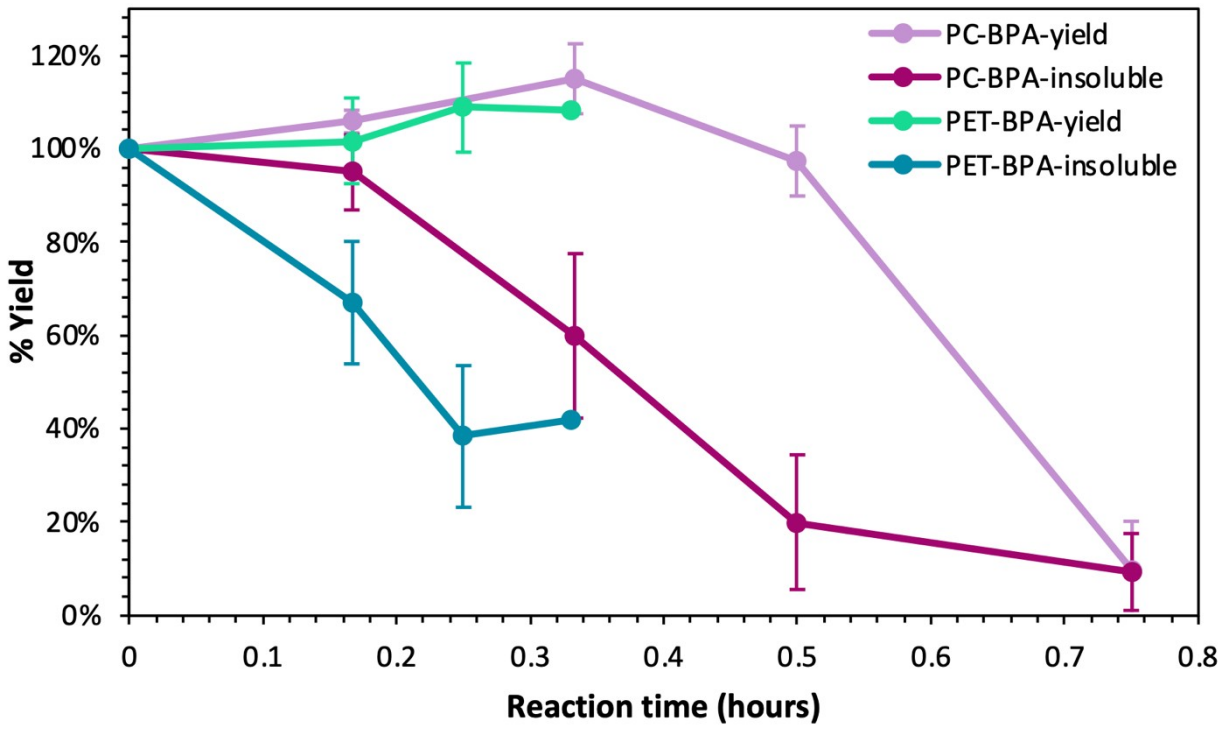

Figure S10 Yield of PET and PC depolymerized with BPA: Change in percent yield of PET and PC as a function of depolymerization time with BPA, including the change in BPA insoluble yield for PET (dark blue) and PC (dark purple). The change in the total yield of BPA soluble and BPA insoluble material as a function of reaction time for PET (blue-green) and PC (light purple) is also shown.

When depolymerizing both polymers with BPA, we isolated BPA-insoluble flakes and BPA-soluble, methanol-insoluble powder. **Figure S11** shows the molecular weights, calculated using SEC GPC, showed that the M_n, M_w, and Đ of BPA-insoluble PET changed over reaction time, as did those of BPA-soluble PET, with Đ increasing with time—unlike depolymerization with EG. Interestingly, substantial molecular weight BPA-soluble PET oligomers were isolated, a phenomenon not seen with EG. Both fractions' molecular weights decreased over time, with the BPA-soluble fraction decreasing faster due to phase similarity with BPA. PET depolymerized in BPA reached a shorter reaction time than when depolymerized in EG, as shown by the decreasing yield of oligomers (**Figure S10**). **Figure S11 (b)** shows similar trends for PC, with Đ of BPA-insoluble PC increasing with time, unlike depolymerization with EG, where Đ decreased for BPA-

soluble PC.

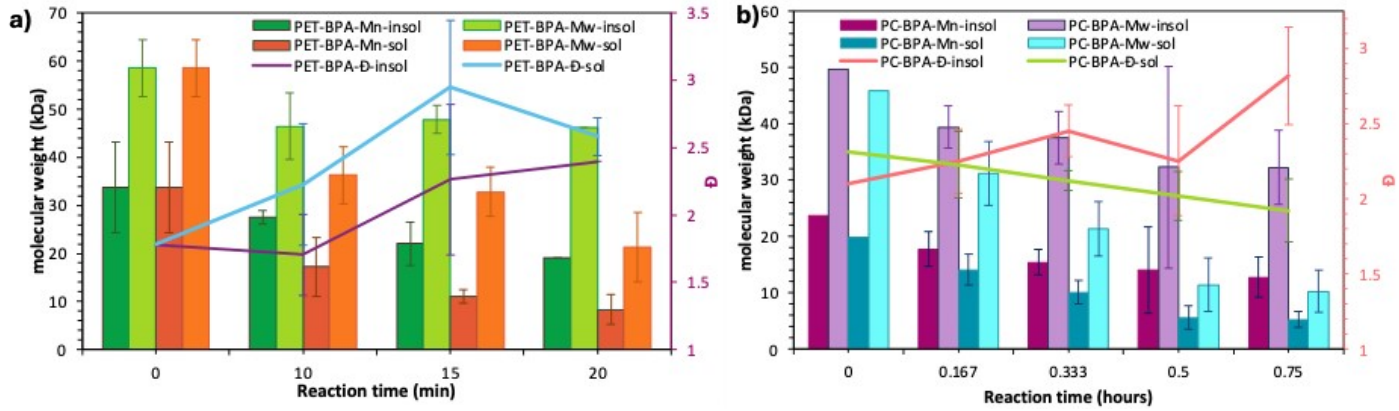

Figure S11 PET and PC depolymerized in BPA. **(a)** shows the change in molecular weight of the insoluble (M_n dark orange, M_w orange) and soluble (M_n dark green, M_w green) fractions of PET with reaction time and the change in dispersity of the insoluble (purple) and soluble fraction (blue). **(b)** shows the change in molecular weight of the insoluble (M_n dark purple, M_w purple) and soluble (M_n dark blue, M_w blue) fractions of PC with reaction time and the change in dispersity of the insoluble (orange) and soluble fraction (green).

Figure S12 shows PET and PC's normalized swelling per polymer flake in BPA. **Figure 4** demonstrates that our amorphous polymer (PC) swells with more EG than our semicrystalline polymer (PET), which is not unexpected.[22] **Figure S12** shows the change in normalized swelling for PET (green line) and PC (pink line) versus the square root of time (minutes). The swelling experiments utilizing BPA were substantially shorter than those utilizing EG as both polymers started to dissolve in BPA faster than in EG. Also, the BPA swelling experiments observed a higher percentage of swelling per polymer flake for both polymers than those using EG. Unexpectantly, this time, the amorphous polymer swells with less solvent than our semicrystalline polymer.

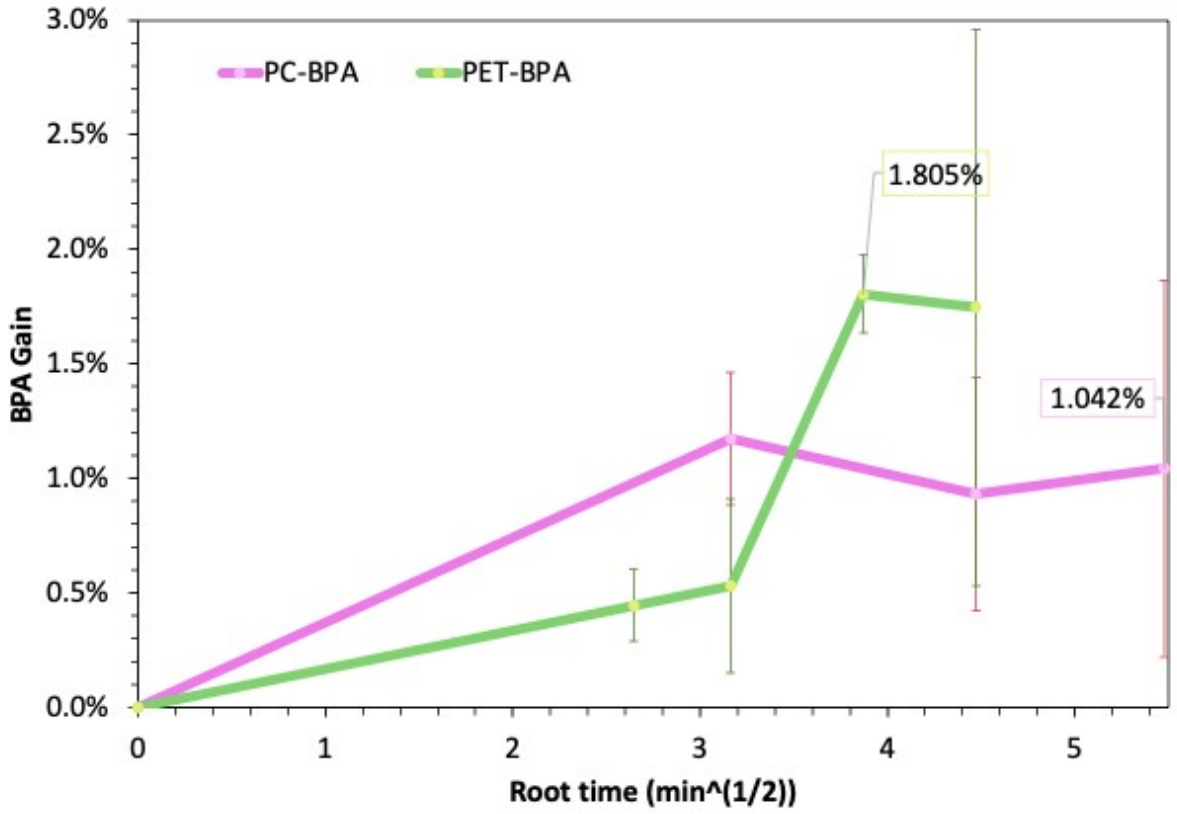

Figure S12 demonstrates the normalized swelling of BPA into PET (green) and PC (pink) versus the square root of time, following Vlachos et al's work.[11]

Figure S13 shows the DSC of PET in varying conditions to understand why semicrystalline PET swells similarly or more than amorphous PC with BPA. When PET is depolymerized (dark blue) or swelled (light blue) with EG, the percent crystallinity increases with time, though the depolymerization mechanism enhances the increase in crystallinity with reaction time. PET annealed at the reaction temperature under vacuum (pink) increases in crystallinity similarly to PET swelled with EG. However, PET depolymerized (red) or swelled (orange) with BPA decreases in crystallinity initially. PET depolymerized with BPA decreases and then increases crystallinity, again demonstrating that the mechanism of the depolymerization aids in crystal growth. However, PET swelled with BPA decreases in crystallinity as it is hypothesized

that BPA disturbs or dissolves the PET crystals, making PET more amorphous and able to swell similarly to PC, as shown in **Figure S12**.

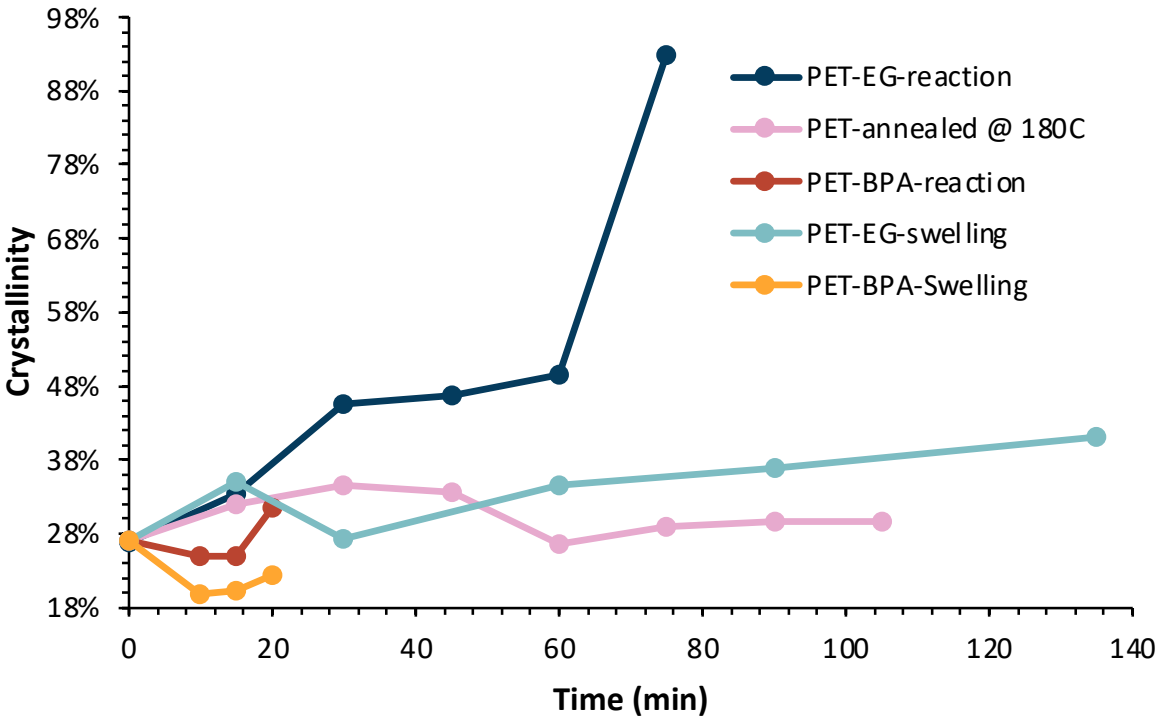

Figure S13 shows the change in percent crystallinity of PET under different conditions (Depolymerized with EG (dark blue), swelled with EG (light blue), annealed at reaction temperature (pink), depolymerized with BPA (red), swelled with BPA (orange) with time.

References

(1) Falkenstein, P.; Gräsing, D.; Bielytskyi, P.; Zimmermann, W.; Matysik, J.; Wei, R.; Song, C. UV Pretreatment Impairs the Enzymatic Degradation of Polyethylene Terephthalate. *Front. Microbiol.* **2020**, *11* (689), Original Research. DOI: 10.3389/fmicb.2020.00689.

(2) Kim, J.; Gracz, H. S.; Roberts, G. W.; Kiserow, D. J. Spectroscopic analysis of poly(bisphenol A carbonate) using high resolution 13C and 1H NMR. *Polymer* **2008**, *49* (2), 394-404. DOI: 10.1016/j.polymer.2007.11.046.

(3) Paul C. Hiemenz, T. P. L. *Polymer Chemistry*; CRC Press, 2007.

(4) Roovers, J.; Toporowski, P. M. Hydrodynamic studies on model branched polystyrenes. *J. Polym. Sci., Polym. Phys. Ed.* **1980**, *18* (9), 1907-1917. DOI: https://doi.org/10.1002/pol.1980.180180904.

(5) Liu, Y.; Yin, L.; Zhao, H.; Song, G.; Tang, F.; Wang, L.; Shao, H.; Zhang, Y. Lamellar and fibrillar structure evolution of poly(ethylene terephthalate) fiber in thermal annealing. *Polymer* **2016**, *105*, 157-166. DOI: https://doi.org/10.1016/j.polymer.2016.10.031.

(6) Chen, Z.; Jenkins, M. J.; Hay, J. N. Annealing of poly (ethylene terephthalate). *Eur. Polym. J.* **2014**, *50*, 235-242. DOI: 10.1016/j.eurpolymj.2013.11.004.

(7) Bhagia, S.; Bornani, K.; Ozcan, S.; Ragauskas, A. J. Terephthalic Acid Copolyesters Containing Tetramethylcyclobutanediol for High-Performance Plastics. *ChemistryOpen* **2021**, *10* (8), 830-841. DOI: 10.1002/open.202100171.

(8) Holdsworth, P. J.; Turner-Jones, A. The melting behaviour of heat crystallized poly(ethylene terephthalate). *Polymer* **1971**, *12* (3), 195-208. DOI: https://doi.org/10.1016/0032-3861(71)90045-0.

(9) Blaine, R. L. *Determination of Polymer Crystallinity by DSC*. TA Instruments, https://www.tainstruments.com/pdf/literature/TA123new.pdf (accessed 2023 07/14/23).

(10) Blaine, R. L. *THERMAL APPLICATIONS NOTE*. TA Instrument, https://www.tainstruments.com/pdf/literature/TN048.pdf (accessed 2023 07/14/23).

(11) Najmi, S.; Vance, B. C.; Selvam, E.; Huang, D.; Vlachos, D. G. Controlling PET oligomers vs monomers via microwave-induced heating and swelling. *Chem. Eng. J.* **2023**, *471*, 144712. DOI: https://doi.org/10.1016/j.cej.2023.144712.

(12) Zhou, X.; Wang, J.; Nie, J.; Du, B. Poly(N-isopropylacrylamide)-based ionic hydrogels: synthesis, swelling properties, interfacial adsorption and release of dyes. *Polym. J.* **2016**, *48* (4), 431-438. DOI: 10.1038/pj.2015.123.

(13) Jehanno, C.; Demarteau, J.; Mantione, D.; Arno, M. C.; Ruipérez, F.; Hedrick, J. L.; Dove, A. P.; Sardon, H. Selective Chemical Upcycling of Mixed Plastics Guided by a Thermally Stable Organocatalyst. *Angew. Chem. Int. Ed.* **2021**, *60* (12), 6710-6717. DOI: 10.1002/anie.202014860.

(14) Jehanno, C.; Flores, I.; Dove, A. P.; Müller, A. J.; Ruipérez, F.; Sardon, H. Organocatalysed depolymerisation of PET in a fully sustainable cycle using thermally stable protic ionic salt. *Green Chem.* **2018**, *20* (6), 1205-1212. DOI: 10.1039/c7gc03396f.

(15) Galan, N. J.; Dishner, I. T.; Sumpter, B. G.; Kertesz, V.; Abdul Rahman, N. B.; Polo-Garzon, F.; Demchuk, Z.; Saito, T.; Foster, J. C. Upcycling of polyethylene terephthalate to high-value chemicals by carbonate-interchange deconstruction. *Green Chem.* **2025**. DOI: 10.1039/d5gc03354c.

(16) Sim, J. H.; Hong, W.; Vu, T. V.; Choi, H.; Kim, J.; Lee, Y.; Kang, Y. Unlocking Hidden Miscibility: Entropy Diluent Strategy for Incompatible Polymer Blends. *Macromol.* **2025**, *58* (18), 9682-9691. DOI: 10.1021/acs.macromol.5c01387.

(17) Jin, L.; Wu, Y.; Kim, C.-K.; Xue, Y. Theoretical study on the aminolysis of ester catalyzed by TBD: Hydrogen bonding or covalent bonding of the catalyst? *Journal of Molecular Structure: THEOCHEM* **2010**, *942* (1-3), 137-144. DOI: 10.1016/j.theochem.2009.12.012.

(18) Hong, M.; Chen, J.; Chen, E. Y. X. Polymerization of Polar Monomers Mediated by Main-Group Lewis Acid–Base Pairs. *Chem. Rev.* **2018**, *118* (20), 10551-10616. DOI: 10.1021/acs.chemrev.8b00352.

(19) Kaiho, S.; Hmayed, A. A. R.; Delle Chiaie, K. R.; Worch, J. C.; Dove, A. P. Designing Thermally Stable Organocatalysts for Poly(ethylene terephthalate) Synthesis: Toward a One-Pot, Closed-Loop Chemical Recycling System for PET. *Macromol.* **2022**, *55* (23), 10628-10639. DOI: 10.1021/acs.macromol.2c01410.

(20) Grabowski, S. J. Hydrogen Bond and Other Lewis Acid–Lewis Base Interactions as Preliminary Stages of Chemical Reactions. *Molecules* **2020**, *25* (20), 4668. DOI: 10.3390/molecules25204668.

(21) Olazabal, I.; Luna, E.; De Meester, S.; Jehanno, C.; Sardon, H. Upcycling of BPA-PC into trimethylene carbonate by solvent assisted organocatalysed depolymerisation. *Polymer Chemistry* **2023**, *14* (19), 2299-2307. DOI: 10.1039/d3py00441d.

(22) Miller-Chou, B. A.; Koenig, J. L. A review of polymer dissolution. *Prog. Polym. Sci.* **2003**, *28* (8), 1223-1270. DOI: 10.1016/s0079-6700(03)00045-5.